

University of Groningen

## Frontal plane roll-over analysis of prosthetic feet

van Hal, Evert S; Curtze, Carolin; Postema, Klaas; Hijmans, Juha M; Otten, Egbert

*Published in:*  
Journal of biomechanics

*DOI:*  
[10.1016/j.jbiomech.2021.110610](https://doi.org/10.1016/j.jbiomech.2021.110610)

**IMPORTANT NOTE: You are advised to consult the publisher's version (publisher's PDF) if you wish to cite from it. Please check the document version below.**

*Document Version*  
Publisher's PDF, also known as Version of record

*Publication date:*  
2021

[Link to publication in University of Groningen/UMCG research database](#)

*Citation for published version (APA):*

van Hal, E. S., Curtze, C., Postema, K., Hijmans, J. M., & Otten, E. (2021). Frontal plane roll-over analysis of prosthetic feet. *Journal of biomechanics*, 125, [110610]. <https://doi.org/10.1016/j.jbiomech.2021.110610>

### Copyright

Other than for strictly personal use, it is not permitted to download or to forward/distribute the text or part of it without the consent of the author(s) and/or copyright holder(s), unless the work is under an open content license (like Creative Commons).

The publication may also be distributed here under the terms of Article 25fa of the Dutch Copyright Act, indicated by the "Taverne" license. More information can be found on the University of Groningen website: <https://www.rug.nl/library/open-access/self-archiving-pure/taverne-amendment>.

### Take-down policy

If you believe that this document breaches copyright please contact us providing details, and we will remove access to the work immediately and investigate your claim.

*Downloaded from the University of Groningen/UMCG research database (Pure): <http://www.rug.nl/research/portal>. For technical reasons the number of authors shown on this cover page is limited to 10 maximum.*



## Frontal plane roll-over analysis of prosthetic feet

Evert S. van Hal<sup>a</sup>, Carolin Curtze<sup>b,\*</sup>, Klaas Postema<sup>c</sup>, Juha M. Hijmans<sup>c</sup>, Egbert Otten<sup>a</sup>

<sup>a</sup> University of Groningen, University Medical Center Groningen, Center for Human Movement Sciences, Groningen, the Netherlands

<sup>b</sup> Department of Biomechanics, University of Nebraska at Omaha, Omaha, NE, USA

<sup>c</sup> University of Groningen, University Medical Center Groningen, Department of Rehabilitation Medicine, Groningen, the Netherlands

### ARTICLE INFO

#### Keywords:

Prosthetic foot curvature  
Material testing  
Mediolateral roll-over  
Frontal/Coronal plane

### ABSTRACT

In prosthetic walking mediolateral balance is compromised due to the lack of active ankle control, by moments of force, in the prosthetic limb. Active control is reduced to the hip strategy, and passive mechanical stability depends on the curvature of the prosthetic foot under load. Mediolateral roll-over curvatures of prosthetic feet are largely unknown. In this study we determined the mediolateral roll-over characteristics of various prosthetic feet and foot-shoe combinations. Characteristics were determined by means of an inverted pendulum-like apparatus. The relationship between the centre of pressure (CoP) and the shank angle was measured and converted to roll-over shape and effective radius of curvature. Further, hysteresis (i.e., lagging in CoP displacement due to material compliance or slip) at vertical shank angle was determined from the hysteresis curve. Passive mechanical stability varied widely, though all measured foot-shoe combinations were relatively compliant. Mediolateral motion of the CoP ranged between 4 mm and 40 mm, thereby remaining well within each foot's physical width. Derived roll-over radii of curvature are also small, with an average of 102 mm. Hysteresis ranges between 20% and 115% of total CoP displacement and becomes more pronounced when adding a shoe. This may be due to slipping of the foot core in its cosmetic cover, or the foot in the shoe. Slip may be disadvantageous for balance control by limiting mediolateral travel of the CoP. It may therefore be clinically relevant to eliminate mediolateral slip in prosthetic foot design.

### 1. Introduction

Compared to able-bodied individuals, lower limb amputees walk with an increased step width. Specifically, on the prosthetic side the foot is placed more lateral with respect to the ground projection of the centre of mass (CoM) (Hof et al., 2007). This is to compensate for the lack of active ankle control, by moments of force, in the prosthetic limb (Hof, 2007; Hof et al., 2007). In able-bodied individuals mediolateral balance control during the stance phase is actively regulated by means of ankle inversion or eversion (ankle moments of force), resulting in mediolateral CoP movements ('lateral ankle strategy'), provided that the support surface is relatively flat, and sufficiently stiff and wide (Hof, 2007; Winter 1995). When the support surface becomes more challenging a gradual increase of 'counter-rotational movements', such as lateral trunk and arm-swing are observed, which result from a hip strategy (Curtze et al., 2010; Curtze et al., 2011; Otten, 1999). The hip joint moments of force ( $T_h$ ) are varied by these movements, thereby modulating the mediolateral component of the ground reaction force ( $F_{ml}$ , see Fig. 1A; Hof, 2007; Otten, 1999; Winter, 1995). Since prosthetic walkers

do not have an active ankle strategy at their disposal, their effective base of support is reduced to a narrow ridge, and the mediolateral CoP travels from posterior to anterior in an almost straight line, even when mediolateral foot placement is actively disturbed (Hof et al., 2007; Segal et al., 2015). This implies that prosthetic walkers can only regulate mediolateral balance during stance on the prosthesis by changing the direction of the mediolateral component of the ground reaction force facilitated by hip moment strategies in the frontal plane.

Currently, no solution is available to compensate for the lack of active ankle mediolateral balance control in prosthetic walking. Any changes in CoP position that do occur are due to the passive mechanics of the prosthetic device (Curtze et al., 2016). Variations in mediolateral CoP occur only when the prosthetic leg rotates in the frontal plane (shank angle  $\theta$ ) in Fig. 1B). The passive mechanical stability of the system is solely determined by the curvature of the foot under load (Curtze et al., 2009), provided no ankle joint with its own passive mechanical properties is present. The curvature is made up of the 1) shape of the unloaded foot, 2) material compliance, and 3) device load. Narrow based, compliant prosthetic feet may exacerbate an already impaired mediolateral balance control.

\* Corresponding author at: Department of Biomechanics, University of Nebraska at Omaha, Omaha, NE 68182, USA.

E-mail address: [ccurtze@unomaha.edu](mailto:ccurtze@unomaha.edu) (C. Curtze).

### Nomenclature

CoM	centre of mass
CoP	centre of pressure, point of attack of ground reaction force
$F_G$	ground reaction force
$F_{ml}$	mediolateral component of ground reaction force.
$l$	pendulum length
$m$	mass
$T_h$	hip moment of force (torque)
$x, y$	x-axis mediolateral, y-axis vertically upward
$x_0$	mediolateral CoP position at $\theta = 0$
$\theta$	tube (shank) angle
$\rho$	radius of curvature

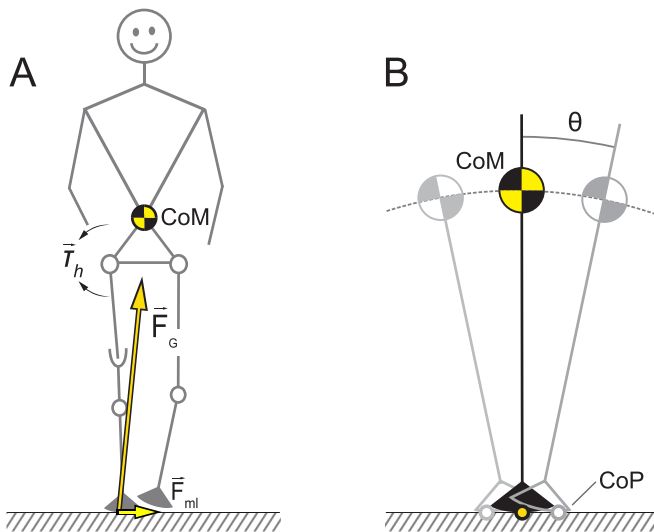


**Fig. 1.** (A) Frontal view showing the orientation of the ground reaction force vector ( $F_G$ ) and its mediolateral component ( $F_{ml}$ ) acting on the CoM at mid-stance as a result of active hip moments of force ( $T_h$ ). (B) Model of the leg as inverted pendulum during mediolateral roll-over over shank angle  $\theta$ . The CoP travels along the curvature of the foot as a function of  $\theta$ .

Passive mediolateral prosthetic foot stability may thus have a considerable effect on residual balance control in prosthetic walking. Yet, the passive mechanical mediolateral stability properties of prosthetic feet are currently unknown. To this purpose, we will measure different types of prosthetic feet and determine their mediolateral roll-over characteristics. Further, we will quantify the effect of different types of shoes on these characteristics.

## 2. Methods

### 2.1. Experimental setup

This paper is an extension of the work on roll-over characteristics of prosthetic feet in the sagittal plane (Curtze et al., 2009). The force acting on a prosthetic limb during the single stance phase was simulated by means of an inverted pendulum like apparatus (Fig. 2). The apparatus consisted of a shaft, with a prosthetic foot attached to the lower end and a mass ( $m$ ) of 70 kg mounted to the upper end of the tube (Curtze et al., 2009). The pendulum length ( $l$ ), i.e., the distance between the foot sole and the CoM of the added weight, was 0.98 m; a typical CoM height for a person of 1.80 m body height (NCD Risk Factor Collaboration, 2020). A

custom-made rig restricting motion to the mediolateral plane provided guidance during roll-over testing with a minimum of friction.

Seven prosthetic feet of three different manufacturers were included in this study: Endolite (Esprit, Navigator), Össur (Talux, Vari-Flex), and Ottobock (1C40, 1D10, 1D35). All feet were right sided with a length of 270 mm. Each prosthetic foot was tested under 4 different conditions: (1) without shoe, (2) with a running shoe, (3) with a men's leather shoe, and (4) with a hiking boot (Fig. 2B).

The prosthetic foot-shoe combinations were mounted in neutral alignment in both the frontal and sagittal plane, i.e. alignment for each shoe was adjusted to accommodate for differences in heel height. Both the feet and the shoes were flat on the ground when the shaft was vertical under zero load. A neutral sagittal plane alignment provides a proxy for the mid stance phase of gait when mediolateral CoP displacement is most relevant: the single support phase. A certified prosthetist orthotist assisted with alignment.

Ground reaction forces were measured with an AMTI force plate, at a sampling frequency of 1000 Hz. Two reflective markers were placed on the shaft, and two on the foot or shoe, representing the heel (calcaneus) and toe (hallux) (Fig. 2). The four markers were tracked by an eight-camera VICON motion analysis system at a sampling frequency of 100 Hz.

### 2.2. Experimental procedure

To facilitate a controlled movement, two experimenters simultaneously applied horizontal forces to the weight mounted to the upper end of the tube, thereby rolling the foot over from lateral to medial and back (Fig. 2). To allow for controlled movement of the 70 kg weight, a rotational velocity of about 10 deg/s was chosen. Anteroposterior movement and pendulum maximum rotational range were controlled for by the custom motion restricting rig. The overall measurement range was around 10–15° from the vertical to both the medial and lateral side. The range variation resulted from inconsistencies due to moving the tube manually. The procedure was repeated three times for each of the foot-shoe combinations, resulting in 3 medial-to-lateral and 3 lateral-to-medial movements.

### 2.3. Data analysis

#### 2.3.1. CoP versus tube angle

Instantaneous CoP and tube angle ( $\theta$ ) were calculated from the force plate and marker data, respectively. Missing values were interpolated with a zero-lag convolution filter at a cutoff frequency of 8 Hz. CoP and tube angle were filtered with a convolution filter at a cutoff frequency of 4 Hz, and subsequently normalized to 2000 data points by cubic spline interpolation. The CoP was then shifted by subtracting the centre of the virtual ankle joint, defined as 1/3 of the line connecting the calcaneus with the toe marker (method adapted from: Oude Lansink et al., 2017). These data were used to depict the relationship between CoP and tube angle over the full range of motion that was tested. The amount of CoP displacement at equal amounts of tube angular displacement, i.e., the CoP -  $\theta$  relationship is an indicator of stability; a larger amount of travel denotes a more stable system (Curtze et al., 2009).

#### 2.3.2. Roll-over shape

During the single support phase, the biological ankle-foot system acts like a smoothly curved solid object to maintain balance in the mediolateral direction. The CoP travels medial to lateral and back, analogous to a rolling wheel with a particular radius. This 'ankle-foot roll-over shape' can be estimated from CoP data (Hansen et al., 2004). This method enables transformation of CoP location data from a laboratory-based coordinate system into a shank-based coordinate system. The ankle-foot roll-over shape resulting from this method is similar to a circle and reflects the mediolateral motion of the system (Hansen et al., 2004).

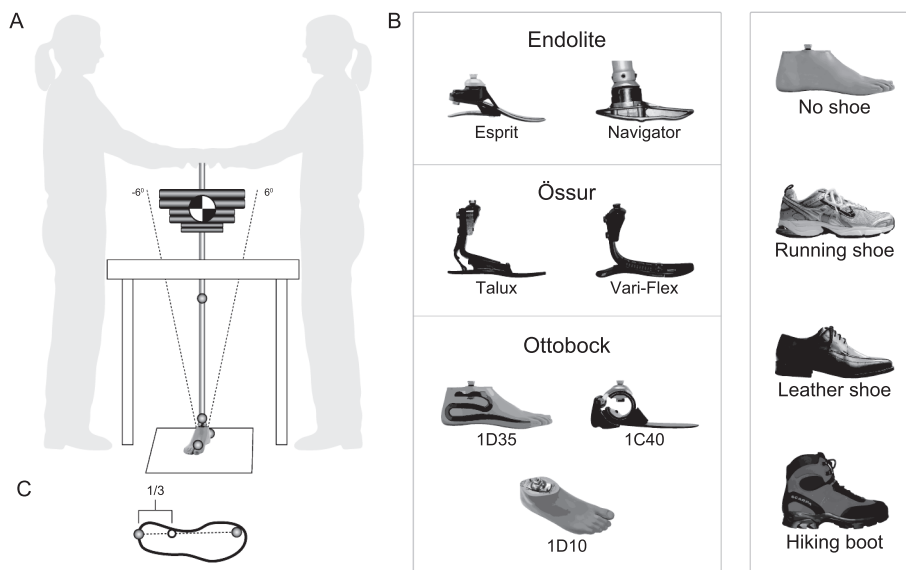


**Fig. 2.** (A) The inverted pendulum-like apparatus. It consists of a prosthetic foot, a shaft, and a 70 kg mass. The CoM of the weight was mounted at a height of 0.98 m. Two reflective markers were placed on the shaft to determine the tube angle. Additionally, a heel and a toe marker were placed on the foot/shoe. The ground reaction forces, and the position of the CoP were measured with a force plate. A custom-made slider rig provided guidance during roll-over. (B) Overview of the prosthetic feet and shoes tested. (C) Planar view of the position of the virtual ankle at 1/3 of the distance between heel and toe marker.

To determine the roll-over shape, the medial to lateral movement was separated from the lateral to medial movement (see 2.3.4). A range from  $-6^\circ$  to  $+6^\circ$  of rotation of the tube angle in 121 steps ( $0.1^\circ/\text{step}$ ) was chosen. The CoP was then resampled by linear interpolation to the new tube angle range. This method corrects for variations in angular velocity during the motion of the pendulum. Subsequently, the medio-lateral foot roll-over shapes' x and y coordinates were obtained by numerical integration of the difference in CoP multiplied respectively by the cosine, and the sine of the tube angle. The successive CoP data were transformed from a laboratory-based into a shank-based coordinate system, as described above (Curtze et al., 2009; Hansen et al., 2004). This way a distinction can be made between the amount of CoP displacement at equal angular displacement, or effective foot 'width', and material compliance of the foot under load, or foot 'flatness'.

### 2.3.3. Effective radius of curvature ( $\rho$ )

The CoP -  $\theta$  relationship can be expressed as the (effective) radius of curvature. A larger effective radius of curvature denotes a more stable system. The effective radius of curvature was calculated by fitting a least-squares, best-fit circular arc to the mediolateral roll-over shapes (Curtze et al., 2009; Hansen et al., 2004).

### 2.3.4. Hysteresis

The direction of tube motion in the apparatus influences the CoP - tube angle ( $\theta$ ) relationship. When comparing the motion from the medial to the lateral side with the motion from the lateral to the medial side hysteresis can be observed. Due to lagging in CoP displacement the CoP position differs at equal tube angles, depending on the motion direction. We defined the difference in CoP positions between motion directions at vertical tube angle as hysteresis.

All data were processed using custom written software in MATLAB (version 9.4). Characteristics are descriptively presented (i.e., as average across all trials for the same condition) to guide future metric selection. No statistical tests were performed.

## 3. Results

### 3.1. CoP versus tube angle

The CoP -  $\theta$  relationship, varies distinctly between feet. Adding a shoe affects the CoP -  $\theta$  relationship for each foot in a different manner. In general, a stiff shoe sole increases CoP displacement at an equal tube angle  $\theta$ , and a more compliant shoe sole decreases CoP displacement,

compared to the no shoe condition. Fig. 3 exemplifies this. Certain inconsistencies exist however, where CoP displacement decreases in all cases when adding a shoe, such as with the Endolite Esprit (Table 1, Fig. 4).

### 3.2. Roll-over shape

Two of the mediolateral roll-over shape examples from Fig. 3 are shown in Fig. 5. Fig. 5C shows a close-up of the amount of roll-over curvature; a combination of the effective foot 'width' (x-coordinate), and compliance under load, or foot 'flatness' (y-coordinate). The Össur Talux with running shoe results in the narrowest overall roll-over shape found, with a total travel of 4.9 mm. The broadest roll-over shape found was that of the Ottobock 1D10 with hiking boot, at 40.9 mm. This denotes a more passive mechanically stable foot. For a complete overview see Table 1. Fig. 4 provides a visual overview of all tested feet and shoe conditions. As with the CoP -  $\theta$  relationship, roll-over widths differ per condition when adding a shoe; in some cases, the foot becomes more stable, while it becomes less stable in other cases (Fig. 4).

### 3.3. Effective radius of curvature ( $\rho$ )

An overview of the radius of curvature for all tested feet, and foot-shoe combinations, can be found in Fig. 6. A larger radius of curvature corresponds with a larger CoP displacement at equal  $\theta$ , and a wider roll-over shape (Fig. 4). Differences in conditions are consistent between these three methods of representation. The average radius of curvature is 102 mm. The 1D10 with a hiking boot has the largest radius of 213 mm (Fig. 6).

The Endolite feet (Esprit, Navigator) and the Össur feet (Vari-Flex, Talux) all show a decrease in radius of curvature when adding shoes. The different types of shoes do not influence the radius much. The Ottobock feet (1D10, 1D35, 1C40) show an increase in the radius of curvature when shoes are added.

### 3.4. Hysteresis

Hysteresis ranges from 3.1 mm to 17.6 mm, with an average of 9.7 mm (Table 1). Hysteresis is illustrated in Fig. 4 as both the varying locations of  $x_0$ , and the percentage of overlap in the drawn horizontal bars (for actual percentages see Table 1). Hysteresis increases in all cases after adding a shoe (Table 1), pushing the directional roll-over shapes further apart (Fig. 4). The increase in hysteresis when a shoe is added is

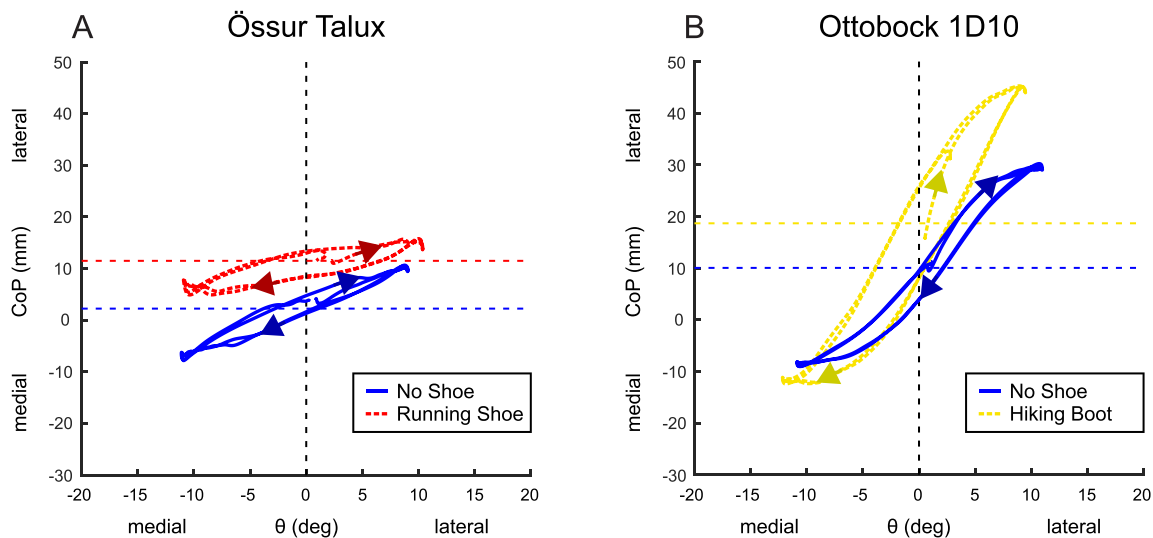


**Fig. 3.** CoP versus tube angle  $\theta$ . Horizontal dotted lines indicate median CoP values. Arrows indicate movement direction. (A) Össur Talux foot without shoe, and with a running shoe. The addition of a running shoe shifts the CoP laterally, decreases total CoP displacement at equal angular displacement, and increases slip. (B) Ottobock 1D10 foot without a shoe, and with a hiking boot. The addition of a hiking boot shifts the CoP laterally, increases CoP displacement at equal angular displacement, and increases slip.

**Table 1**

Overview of all tested feet and foot-shoe conditions.

Foot Model	Shoe Type	CoP displacement (mm) <sup>a</sup>	CoP overlap (%) <sup>a</sup>	Hysteresis range (mm)	Hysteresis/CoP displacement (%)
Ottobock 1D10	Hiking boot	40.90	75.7	17.62	43.1
	Leather shoe	33.71	80.9	11.45	34.0
	Running shoe	37.01	78.5	14.79	40.0
	No shoe	28.71	88.4	5.61	19.5
Össur Vari-Flex	Hiking boot	20.35	37.6	16.47	81.0
	Leather shoe	23.37	64.7	12.30	52.6
	Running shoe	19.88	53.6	14.52	73.0
	No shoe	24.86	84.5	5.43	21.8
Endolite Esprit	Hiking boot	16.43	50.6	8.47	51.6
	Leather shoe	14.58	36.6	10.13	69.5
	Running shoe	16.35	61.3	7.72	47.2
	No shoe	21.51	92.0	3.37	15.7
Ottobock 1C40	Hiking boot	24.81	57.1	14.51	58.5
	Leather shoe	25.02	67.0	10.07	40.2
	Running shoe	19.78	53.1	11.04	55.8
	No shoe	19.39	85.1	5.91	30.5
Ottobock 1D35	Hiking boot	27.84	73.5	12.30	44.2
	Leather shoe	27.73	73.0	9.63	34.7
	Running shoe	23.76	63.7	11.35	47.8
	No shoe	18.13	79.6	5.34	29.4
Endolite Navigator	Hiking boot	13.83	24.7	12.70	91.9
	Leather shoe	10.87	30.7	12.51	115.0
	Running shoe	11.29	33.9	10.48	92.8
	No shoe	15.28	61.7	8.96	58.6
Össur Talux	Hiking boot	7.25	34.3	5.31	73.2
	Leather shoe	7.13	37.7	5.16	72.3
	Running shoe	4.88	24.3	4.66	95.5
	No shoe	10.09	77.8	3.11	30.9

<sup>a</sup> Average of both movement directions.

generally larger for stiffer feet, such as the Vari-Flex and 1D10, showing an increased hysteresis of over 10 mm when a hiking boot is added. The hysteresis range (difference in max and min hysteresis values at vertical tube positions of both movement directions) approaches and even exceeds the total CoP displacement for certain foot-shoe combinations, for instance with the Össur Talux and Endolite Navigator (Table 1). The

Endolite Navigator is fitted with a ‘snubber’ ball; a rubber ball joint between tube and foot designed to give the user some slack in the transversal plane while walking. Found hysteresis values for this foot may therefore be larger than expected based on foot properties alone.

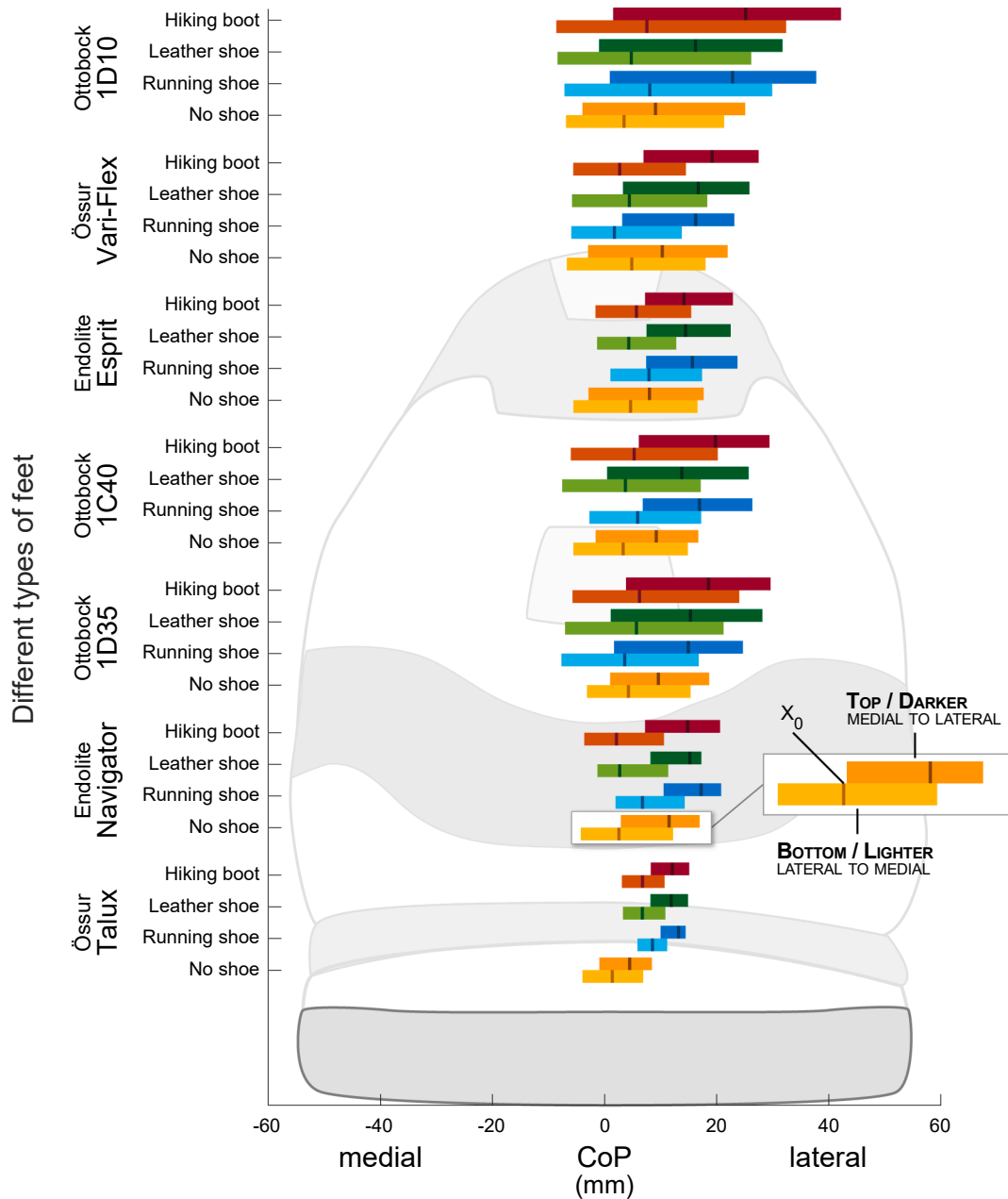


**Fig. 4.** Schematic overview of all tested feet and shoe conditions, sorted from largest (top) to smallest (bottom) roll-over width in the no shoe conditions. A dark mark ( $x_0$ ) denotes the vertical. The bar represents the CoP displacement of the  $-6^\circ$  to  $+6^\circ$  tube range. Differences in contrast indicate movement direction and are due to hysteresis (Fig. 7).

#### 4. Discussion

Passive mechanical mediolateral roll-over testing of various prosthetic feet and foot-shoe combinations revealed a wide range of stability properties. Though compliance varies greatly between all tested prosthetic feet, all mediolateral roll-over widths are relatively small, and remain well within each foot’s physical width. Since foot or shoe sole shapes are roughly flat, and load is comparable to that of average human body weight, the small radii of curvature (Fig. 6) are most likely due to large material compliance. Compliance thus reduces the functional base of support of a prosthetic foot, and with it the foot surface width used during mediolateral roll-over.

This study provides a straightforward method to determine the passive mechanical (mediolateral) characteristics of different prosthetic feet and foot-shoe combinations. Testing occurred in a fixed sagittal

plane angle, resembling mid-stance. Mediolateral roll-over curves may vary throughout the gait cycle depending on foot sagittal angle. It may be clinically meaningful to obtain mediolateral roll-over shapes of various fixed anteroposterior foot angles representing typical stance phases during gait.

A compliant passive mechanical prosthetic foot may not necessarily be disadvantageous for active mediolateral balance control. Shell et al. (2017) reported that mediolateral balance control in unilateral amputee walkers improved with increasing compliance of the prosthetic foot. Segal and Klute (2014) found no significant differences in recovery response after a mediolateral perturbation between a stiff and a more compliant prosthetic foot, concluding that a stiffer prosthetic foot does not help mitigate fall risk. In a follow-up study, the authors conclude that recovery strategies differ minimally between the stiff and more compliant foot (Segal et al, 2015). This suggests that mediolateral



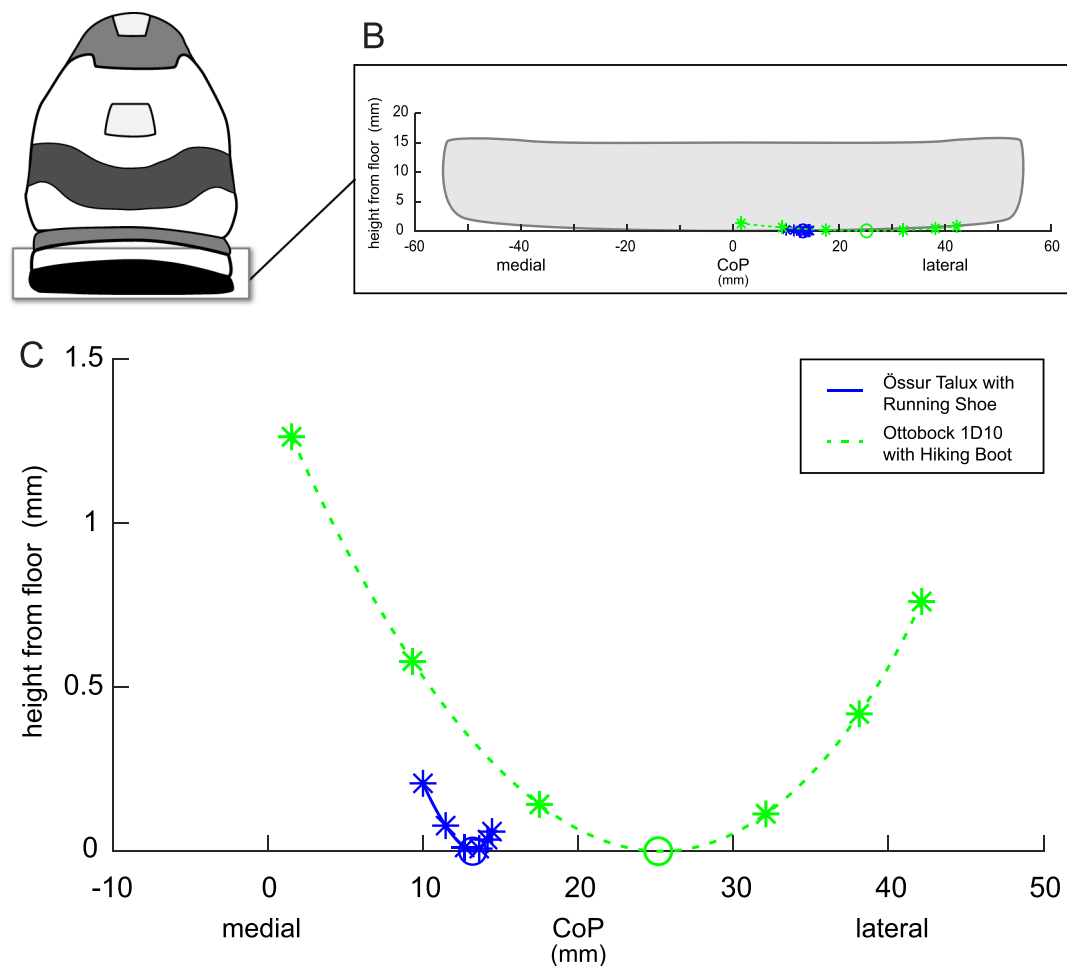


**Fig. 5.** Medial to lateral roll-over shape examples. (B) Roll-over shapes superimposed on a foot sole. (C) Close-up of the roll-over shapes, without equal axes magnitudes. An 'O' denotes the vertical, corresponding with  $x_0$  in Fig. 4. Each asterisk (\*) represents a 2-degree rotation of the tube. Note the difference in compliance (height from floor) between the two feet.

prosthetic foot compliance is less important than the ability to efficiently control the  $F_{ml}$  (i.e., a hip strategy) during the stance phase on the prosthetic foot.

Relevant optima of prosthetic foot shape and compliance with respect to mediolateral balance control during walking remain unknown. It is important to determine optimal -anteroposterior and mediolateral- roll-over characteristics of prosthetic feet during gait, considering the preferences of the target population. Regardless of individual wishes, shoe and cosmetic cover fitting should be taken into consideration when designing prosthetic feet. Total compliance may increase if the shoe sole is more compliant than the foot, and vice versa, but since compliance properties of the shoe soles were not tested in this study, this remains to be determined.

In the no shoe condition, directionally dependent CoP shifts are mostly due to material hysteresis (Fig. 7). Hysteresis becomes more pronounced when adding a shoe (Figs. 3 and 4), most likely due to the addition of an extra layer of elastic material (rubber sole). Hysteresis expressed as a range can even exceed total CoP displacement. Even for stiff feet, hysteresis takes up a large portion of the total CoP displacement found. A substantial reduction in (CoP) overlap of the two movement directions (medial to lateral, lateral to medial) can be seen in most feet, except those by Ottobock (Fig. 4; Table 1). Additionally, the radius of curvature diminished in the respective foot-shoe combinations (Fig. 6). This is most likely due to slip between the foot core and the cosmetic cover, resulting from the foot core -partially- slipping in the cosmetic cover, and/or the foot in the shoe. Close visual inspection of

the video recordings confirmed that the shoe does not rotate along with the tube in those feet. In other words, the shoe and cosmetic cover together form a loose connection with the foot core. Since this effect is less pronounced with the tested feet made by Ottobock, we assume that these particular feet have a tighter fit between the foot core and the cosmetic cover. The observed slip may be disadvantageous for passive mediolateral stability efficacy. Future studies should aim to confirm ecological validity, i.e., determine if the slip found during mechanical testing in this study is consistent with slip during prosthetic walking. During the prosthetic stance phase of walking a hip strategy, i.e., exerting hip moments of force to control the  $F_{ml}$ , is key to controlling the direction of the fall, since the ankle strategy is not available. Hysteresis and slip may delay or diminish the point of application of those hip moments of force on the foot around its longitudinal axis, which may adversely affect active mediolateral balance control. Foot hysteresis may also confound testing. Since material choices influence hysteresis, a careful consideration of materials used in prosthetic design is warranted.

With the current measurement setup distinctions cannot be made between hysteresis and slip of both the bare prosthetic foot, and the foot-shoe combinations. To determine rate-dependent hysteresis, the current method may be expanded to incorporate multiple constant rotational velocities. A velocity dependent constant can thus be determined. To identify the amount of slip, measurements can be performed twice: with and without the components fixated, e.g., by gluing foot core and cosmetic cover, and/or feet and shoes together. Slip may also be velocity dependent, so these measurements should be performed on multiple

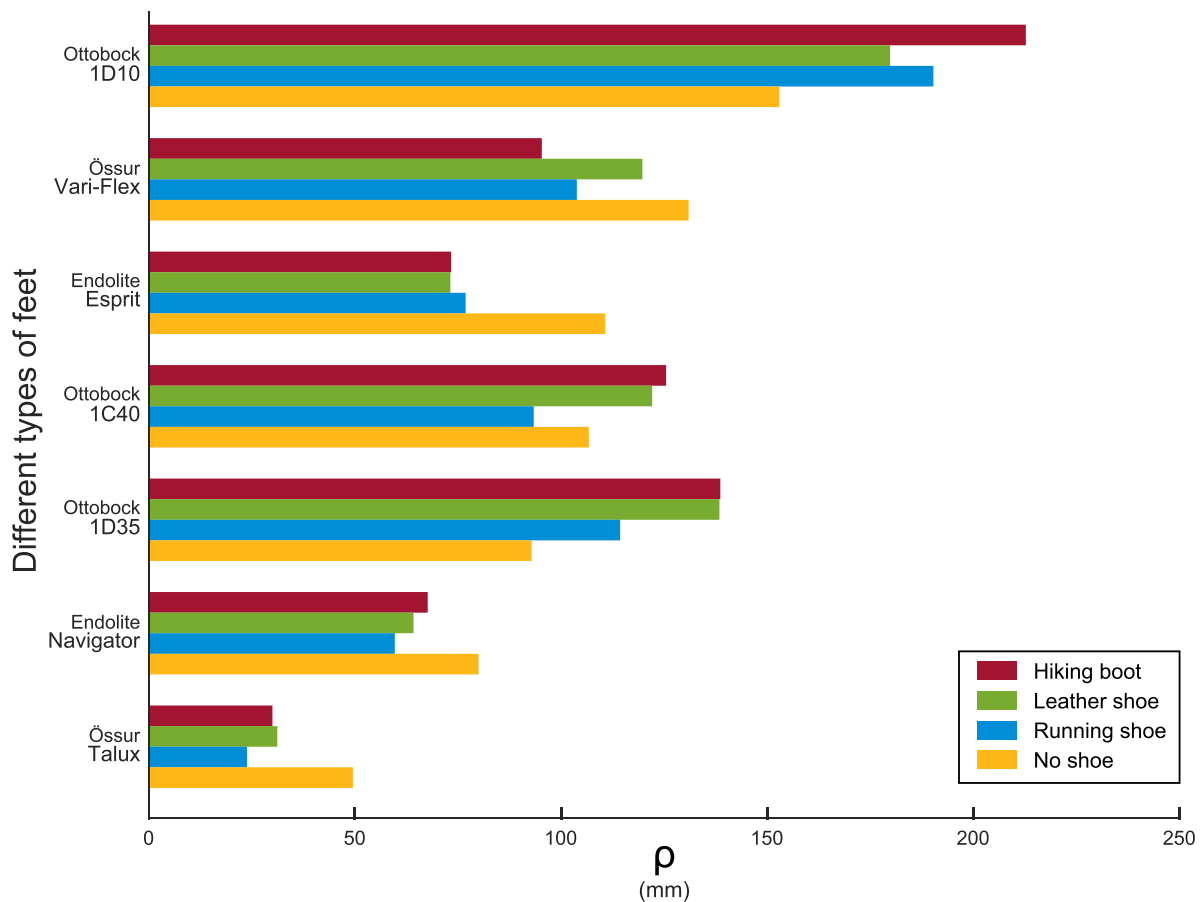


**Fig. 6.** Effect of different feet and shoes combinations on the radius of curvature sorted by no shoe condition from large to small. A larger radius denotes a more stable foot. Note that a larger radius corresponds with a wider bar in Fig. 4.

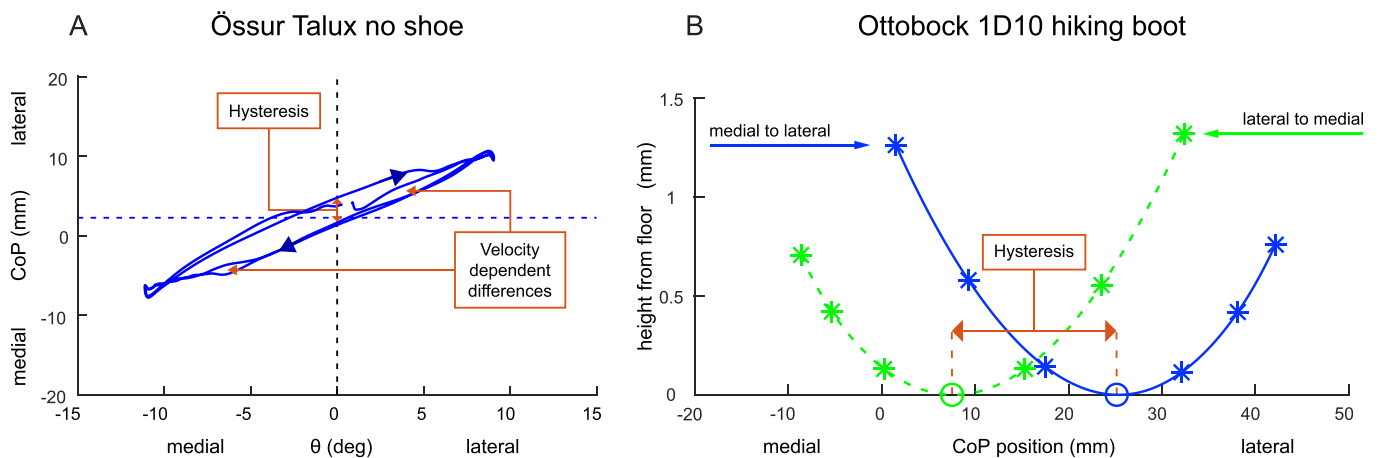


**Fig. 7.** Hysteresis. Depending on movement direction different CoP locations exist at equal tube angles  $\theta$ . (A) CoP versus tube angle  $\theta$  of the Össur Talux, without a shoe (Close-up of Fig. 3A). Note the velocity dependent differences in the curve, on multiple locations throughout the movement. (B) Roll-over shape of the Ottobock 1D10 with a hiking boot.

constant rotational velocities as well. Since we only measured a small selection of feet and shoes, it would be valuable to extend measurements, perhaps by creating a database consisting of many feet under varying loads, rotational velocities, orientations, and phases of the gait cycle.

In conclusion, prosthetic feet display a wide range of mediolateral roll-over characteristics, for which our pendulum-like apparatus provides a precise, and repeatable measuring method. The addition of

different shoes modulated these mediolateral roll-over characteristics slightly, making the foot-shoe combination less or more stable depending on the presence or absence of slip, respectively. Slip may be disadvantageous for balance control by limiting mediolateral travel of the CoP, thereby nullifying passive mechanical stability efficacy. It may therefore be important to eliminate mediolateral slip in prosthetic design.



## Declaration of Competing Interest

The authors declare that they have no known competing financial interests or personal relationships that could have appeared to influence the work reported in this paper.

## Acknowledgments

This study has been performed on behalf of research centre SPRINT, financed by the alliance of Northern Netherlands (SNN), [grant number T1015]. Carolin Curtze was supported by the Centers of Biomedical Research Excellence grant [P20GM109090] from NIGMS/NIH, and by a NASA EPSCoR grant [80NSSC18M0076].

## References

- Curtze, C., Hof, A.L., Postema, K., Otten, B., 2011. Over rough and smooth: amputee gait on an irregular surface. *Gait Posture* 33, 292–296. <https://doi.org/10.1016/j.gaitpost.2010.11.023>.
- Curtze, C., Hof, A.L., Postema, K., Otten, B., 2016. Staying in dynamic balance on a prosthetic limb: a leg to stand on? *Med. Eng. Phys.* 38, 576–580. <https://doi.org/10.1016/j.medengphy.2016.02.013>.
- Curtze, C., Hof, A.L., van Keeken, H.G., Halbertsma, J.P.K., Postema, K., Otten, B., 2009. Comparative roll-over analysis of prosthetic feet. *J. Biomech.* 42, 1746–1753. <https://doi.org/10.1016/j.jbiomech.2009.04.009>.
- Curtze, C., Postema, K., Akkermans, H.W., Otten, B., Hof, A.L., 2010. The Narrow Ridge Balance Test: a measure for one-leg lateral balance control. *Gait Posture* 32, 627–631. <https://doi.org/10.1016/j.gaitpost.2010.09.005>.
- Hansen, A.H., Childress, D.S., Knox, E.H., 2004. Roll-over shapes of human locomotor systems: effects of walking speed. *Clin. Biomech.* 19, 407–414. <https://doi.org/10.1016/j.clinbiomech.2003.12.001>.
- Hof, A.L., 2007. The equations of motion for a standing human reveal three mechanisms for balance. *J. Biomech.* 40, 451–457. <https://doi.org/10.1016/j.jbiomech.2005.12.016>.
- Hof, A.L., van Bockel, R.M., Schoppen, T., Postema, K., 2007. Control of lateral balance in walking. Experimental findings in normal subjects and above-knee amputees. *Gait Posture* 25, 250–258. <https://doi.org/10.1016/j.gaitpost.2006.04.013>.
- NCD Risk Factor Collaboration (NCD-RisC), 2020. Height and body-mass index trajectories of school-aged children and adolescents from 1985 to 2019 in 200 countries and territories: a pooled analysis of 2181 population-based studies with 65 million participants. *Lancet* 396, 1511–1524. [https://doi.org/10.1016/S0140-6736\(20\)31859-6](https://doi.org/10.1016/S0140-6736(20)31859-6).
- Otten, E., 1999. Balancing on a narrow ridge: biomechanics and control. *Philos. Trans. R. Soc. Lond., B Biol. Sci.* 354, 869–875. <https://doi.org/10.1098/rstb.1999.0439>.
- Oude Lansink, I.L.B., van Kouwenhove, L., Dijkstra, P.U., Postema, K., Hijmans, J.M., 2017. Effects of interventions on normalizing step width during self-paced dual-belt treadmill walking with virtual reality, a randomised controlled trial. *Gait Posture* 58, 121–125. <https://doi.org/10.1016/j.gaitpost.2017.07.040>.
- Segal, A.D., Klute, G.K., 2014. Lower-limb amputee recovery response to an imposed error in mediolateral foot placement. *J. Biomech.* 47, 2911–2918. <https://doi.org/10.1016/j.jbiomech.2014.07.008>.
- Segal, A.D., Shofer, J.B., Klute, G.K., 2015. Lower-limb amputee ankle and hip kinetic response to an imposed error in mediolateral foot placement. *J. Biomech.* 48, 3982–3988. <https://doi.org/10.1016/j.jbiomech.2015.09.014>.
- Shell, C.E., Segal, A.D., Klute, G.K., Neptune, R.R., 2017. The effects of prosthetic foot stiffness on transtibial amputee walking mechanics and balance control during turning. *Clin. Biomech.* 49, 56–63. <https://doi.org/10.1016/j.clinbiomech.2017.08.003>.
- Winter, D., 1995. Human balance and posture control during standing and walking. *Gait Posture* 3, 193–214. [https://doi.org/10.1016/0966-6362\(96\)82849-9](https://doi.org/10.1016/0966-6362(96)82849-9).